D5

Preceding page blank

CHARACTERISTICS OF WING SECTIONS AT SUBCRITICAL SPEEDS

By Albert E. von Doenhoff and Laurence K. Loftin, Jr.

Langley Aeronautical Laboratory

The characteristics of wing sections at subcritical speeds have been the subject of intensive research since the airplane was first invented. The problem has been attacked both experimentally and theoretically. As a result of these investigations, we have today a qualitative understanding of nearly all the flow phenomena associated with the various characteristics and we are able to calculate many of the characteristics theoretically. The present paper represents an attempt to summarize briefly some of the more important aspects of our theoretical and experimental knowledge of the flow about airfoil sections and to indicate the way in which this knowledge was used in the design of NACA 6-series or low-drag airfoils. Acknowledgement is gratefully expressed for the expert guidance and many original contributions of Mr. Eastman N. Jacobs, who supervised much of the experimental work to be discussed and the application of the theoretical methods to the design of improved airfoil sections.

One of the concepts most useful in understanding the behavior of airfoil sections is that of the thin airfoil. For the purpose of determining the chordwise load distribution at various angles of attack, and hence the angle of zero lift, the slope of the lift curve, and the pitching-moment coefficient, the airfoil is considered to be replaced by a curved line that is midway between the upper and lower surfaces of the airfoil; that is, the airfoil is considered to be replaced by its mean line. The usual form of mean-line theory as developed by Munk, Birnbaum, Glauert, Theodorsen (references 1 to 5) and others assumes that the angle of attack is small and that the slopes and ordinates are sufficiently small that all effects of these quantities are proportional to their magnitude. In other words, the mean-line theory is a linearized theory. For the purposes of the theory, the air is assumed to be nonviscous and incompressible.

The basic relations of thin-airfoil theory are given in figure 1. Abscissas and ordinates are represented by x and y, respectively. The vertical component of induced velocity is v, the free-stream velocity is V, and the angle of attack is α. Circulation of strength γ per unit length is assumed to be distributed along the mean line. This circulation per unit length is equal to the difference in tangential components of velocity between the upper and lower surfaces. Equation (1) in figure 1 states that the flow must be tangential to the surface, that is, there can be no flow through the mean line. Equation (2) is a formula for calculating the vertical component of induced velocity at any station x_0 in terms of the distribution of circulation along the chord. A problem can be solved by simultaneous solution of equations (1) and (2) either by finding the distribution of γ associated with a given mean line at a given angle of attack, or by finding the mean line for a given distribution of γ.

Most practical airfoil sections are sufficiently thin that the approximations of mean-line theory hold with good accuracy. Numerous comparisons between theoretical and experimental results are available in the literature for many types of airfoil sections. (See references 6 and 7.) In general, good agreement can be expected except in cases where the flow has separated from the surface of the airfoil, as at high angles of attack, large flap deflections, and so forth.

In spite of the many useful results obtained from thin-airfoil or mean-line theory, the nature of the information required for a particular problem may frequently be beyond the scope of this simplified approach. No information, of course, is given concerning the actual distribution of pressure over the surfaces of an airfoil, and as will be pointed out later, such information is necessary for the design of improved airfoil sections. In order to be able to compute the actual pressure distribution about an airfoil, as opposed to the calculation of the chordwise loading, the more elaborate methods of thick-airfoil theory must be used. This theory as developed by Theodorsen and Garrick (references 8 and 9) is a rigorous treatment of the problem of finding the perfect-fluid pressure distribution about an airfoil of arbitrary shape. The method consists essentially of finding suitable conformal transformations to relate the known flow about a circle to the unknown flow about the airfoil. An analysis made by Joukowski which permits the direct transformation of the flow about a circle into the flow about a particular type of airfoil, called a Joukowski airfoil, has been known for a long time. In the Theodorsen method, as shown in figure 2, the Joukowski transformation $\zeta = Z' + \frac{a^2}{Z'}$ is applied, in reverse, to the arbitrary airfoil. Since all airfoils can be roughly approximated by a Joukowski airfoil of about the same thickness, the application of the Joukowski transformation to the arbitrary airfoil (ζ-plane) results in a nearly circular curve in the Z'-plane, the equation of which is given by the relation $Z' = ae^{(\psi+i\theta)}$. According to the Reimann theorem, any simple closed curve can be transformed into a circle. Theodorsen found a particularly convenient process for accomplishing this result. By a process of successive approximations, the first one or two steps of which are generally sufficient in practice, the distorted circle is transformed into a true circle whose equation is $Z = ae^{(\psi_0+i\phi)}$ where ψ_0 is a constant. The transformation is given by $\frac{Z'}{Z} = e^{\left[(\psi-\psi_0)+i(\theta-\phi)\right]}$, where the quantities $(\psi - \psi_0)$ and $(\theta - \phi)$ represent the radial and angular distortions between corresponding points in the near- and true-circle planes. The flow about the arbitrary airfoil is found by applying these transformations in reverse order to the known field of flow about the true circle.

A comparison between the pressure distribution found experimentally and that computed by the Theodorsen method at a low angle of attack is given in figure 3. (See also reference 7.) The solid line is the result of the theoretical calculation and the test points represent the experimental results.

At higher angles of attack and lift coefficients, the agreement between theory and experiment is generally not so close. This is due to the formation of a relatively thick boundary layer primarily along the rear portion of the upper surface. Under such conditions, the angle of attack at which a given lift coefficient is obtained experimentally is not the same as the theoretical angle of attack. Pinkerton (reference 10) found that it was possible to obtain nearly perfect agreement between measured and calculated pressure distributions by reducing the theoretical circulation at a given angle of attack to the value corresponding to the measured lift coefficient and then modifying the trailing-edge shape in such a manner that the Kutta-Joukowski condition is satisfied. The modification of the airfoil shape corresponded closely to the estimated change in the effective shape of the airfoil caused by the thickening of the boundary layer.

It is often desirable to determine the effects of airfoil thickness, thickness form, and type and amount of camber on the pressure distribution for large numbers of airfoils. Such calculations could, of course, be carried out by using the Theodorsen method for each individual case. The amount of computational labor involved in such a procedure, however, would probably be excessive. Great simplification of methods for calculating airfoil pressure distributions approximately was made possible by the work of Allen which showed that the effects of thickness form and load distribution could be considered separately. (See reference 11.)

The method is based essentially on the assumption that the velocity distribution about an airfoil may be approximated by the following three independent components (see fig. 4):

(1) The velocity over the symmetrical airfoil at zero angle of attack (thickness). This velocity distribution can be obtained by the Theodorsen method as previously discussed.

(2) The incremental velocity distribution corresponding to the load distribution of the mean line at the design lift coefficient (camber). The design lift coefficient is the lift coefficient at which the flow enters the leading edge of the mean line smoothly. This type of incremental velocity distribution is a function only of the mean-line geometry and can be obtained by the methods of thin-airfoil theory.

(3) The additional type of incremental velocity distribution associated with departure of the angle of attack or lift coefficient from the design conditions (angle). This type of velocity distribution is, according to thin-airfoil theory, independent of airfoil geometry and depends only on this departure of the angle of attack. The additional type of velocity distribution obtained from thin-airfoil theory is of limited practical application, however, because this simple theory leads to infinite values of the velocity at the leading edge. This difficulty, together with the slight dependence of the additional velocity distribution on airfoil

shape, is taken into account by calculating the velocity increments for each symmetrical airfoil by the methods of thick-airfoil theory.

The final pressure distribution at an arbitrary angle of attack is found by summing the three components of velocity: $S = \left(\frac{v}{V} \pm \frac{\Delta v}{V} \pm \frac{\Delta v_a}{V}\right)^2$. The plus sign is used for the upper surface and the minus sign for the lower surface. The final diagram in figure 4 shows the results of summing the various components of the pressure distribution. The short-dash line represents the pressure distribution about the symmetrical airfoil at zero lift. The long-dash line gives the pressure distribution about the cambered airfoil at the design lift coefficient. The solid line gives the pressure distribution about the cambered section at a lift coefficient higher than the design value.

The convenience of this method of calculating the pressure distribution is primarily due to the availability of tabulated values of the necessary component velocity distributions for large numbers of symmetrical airfoils and mean lines. (See reference 7.)

Although the theories just discussed permit the calculation of a number of airfoil characteristics with good accuracy, since they are essentially based on the concept of a perfect fluid, they give no direct information about one of the most important airfoil characteristics, namely, the drag. As will be shown later, however, these theories have proved invaluable in the design of low-drag airfoil sections. Another important characteristic about which no direct theoretical information has been obtained is the maximum lift coefficient. Some discussion of the maximum lift coefficient will be given in a paper by Sivells entitled "Maximum-Lift and Stalling Characteristics of Wings." The present discussion is concerned primarily with the drag.

From 1929 to 1937, extensive experimental investigations were made of families of related airfoil sections in the NACA variable-density wind tunnel. (See references 6 and 12 to 15.) A large amount of information on the drag was accumulated in these investigations. In figure 5 are shown typical drag data at a low lift coefficient for one of the airfoils tested. (See reference 14.) The drag coefficient c_d is plotted as a function of Reynolds number R. The upper line is the drag coefficient for a flat plate with completely turbulent boundary-layer flow. The lower line is the drag coefficient for a flat plate with completely laminar flow. The comparison between the airfoil drag data and the flat-plate skin friction indicates that nearly all the profile drag is attributable to skin friction. Comparisons, such as this, made it apparent that any pronounced reduction of the profile drag must be obtained by a reduction of the skin friction through increasing the relative extent of the laminar boundary layer. Theoretical and experimental work on this problem was begun late in 1937.

The basic requirement for obtaining extensive regions of laminar flow is that the pressure continuously decreases in the direction of flow throughout the region in which laminar flow is expected. This requirement necessitated the development of methods which would permit the design of airfoil sections having specified types of pressure distribution. The method developed consists of a process of successive approximations in which the ordinates and corresponding pressure distribution are calculated with a high degree of accuracy. The pressure-distribution characteristics thus obtained are compared with the characteristics desired. The nature of the Theodorsen relations (shown in fig. 2) for thick airfoils is such that it is not feasible to express the airfoil velocity distribution directly as a function of the airfoil coordinates. There are, however, relatively simple relations between the distortion parameters $(\psi - \psi_0)$ and $(\theta - \phi)$ relating the near and true circles and the airfoil coordinates on one hand, and between these distortion parameters and the airfoil velocity distribution on the other hand. (See reference 5.) The airfoil coordinates and corresponding velocity distribution were, therefore, calculated from assumed values of the distortion parameters. The choice is subject to certain simple conditions that insure closed symmetrical shapes for the basic thickness forms. (See reference 7.) Approximate relations were found by means of which it is possible to modify successively the original choice of parameters so as to yield airfoils having the desired type of velocity distribution. (See references 7 and 16.) Another method of solving this problem has been developed by Goldstein and was described in his recent Wright Brothers lecture. (See reference 17.)

A typical pressure distribution for one of the low-drag airfoils derived is shown in figure 6. It was noted previously that the type of loading resulting from changes in angle of attack tends to make the pressures along one of the airfoil surfaces increase in the direction of flow. Because of the desirability of obtaining low drag over a range of lift coefficient, the magnitude of the favorable pressure gradient over the forward part of the basic thickness form at zero lift should, therefore, be greater than that of the unfavorable gradient corresponding to the additional type of loading throughout a reasonable range of lift coefficient The requirements of a wide low-drag range, good characteristics at high subsonic speeds, and good maximum-lift characteristics are somewhat conflicting. These conflicting requirements place an upper limit on the magnitude of the low-drag range of lift coefficient for which the airfoil should be designed. The optimum form for the pressure distribution is such that at the extremities of the low-drag range of lift coefficient, the pressure gradient on the suction side of the airfoil becomes substantially flat from a point near the leading edge to the original position of minimum pressure. For the airfoil shown in figure 6, this condition exists at a lift coefficient of 0.22. A more complete discussion of the problem of finding the proper type of pressure distribution is given in reference 7.

The desirability of obtaining low drag corresponding to extensive laminar flow at lift coefficients higher than those possible with the basic

thickness form alone indicated the necessity for mean camber lines which would shift the low-drag range to higher values of the lift coefficient, but which would not at the same time decrease the range of lift coefficient for low drag. These requirements define a type of mean line that has, at design conditions, a uniform chordwise distribution of load at least as far back as the position of minimum pressure on the basic thickness form. The method of deriving mean lines to have such prescribed load distributions employs the previously discussed thin-airfoil theory, and is relatively simple compared with the more usual problem of finding the load distribution corresponding to a given mean line.

By the use of the theoretical methods discussed, a large number of related airfoil sections designed for extensive laminar flow were derived. Some method of designating members of this group of airfoils is necessary. The NACA method can be explained by the designation shown in figure 6:

NACA 64_2-015

The first digit is merely a series designation. The second digit gives the position of minimum pressure on the basic thickness form at zero lift in tenths of the chord measured from the leading edge. The subscript gives the range of lift coefficient on either side of the design lift coefficient through which the pressure gradients on both surfaces are favorable for laminar flow. The first digit following the dash gives the design lift coefficient in tenths. (In this case, since the airfoil is symmetrical, the value is 0.) The last two digits give the thickness ratio in percent of the chord.

Approximately 100 of these related airfoils were investigated experimentally. (See reference 7.) In order actually to achieve extensive laminar flow at high Reynolds numbers, it is necessary that the turbulence level of the wind-tunnel air stream be extremely small so as to simulate flight conditions correctly. A description of the development of low-turbulence wind tunnels is given in recent papers by Dryden and Schubauer (reference 18) and Von Doenhoff and Abbott (reference 19).

Some of the results obtained from the experimental investigation of NACA 6-series airfoils are presented in the next few figures. The value of the drag coefficient in the low-drag range for smooth airfoils is mainly a function of the Reynolds number and the relative extent of the laminar layer and is moderately affected by the airfoil thickness ratio and camber. The effect on minimum drag of the position of minimum pressure, which determines the possible extent of laminar flow, is shown in figure 7 for some NACA 6-series airfoils. (See reference 7.) The data show a regular decrease in drag coefficient with rearward movement of minimum pressure. Also shown in this figure is the minimum drag coefficient of the older NACA 2415 airfoil section. Comparison shows that savings in minimum drag of from 20 percent to 50 percent, depending upon the position of minimum pressure, are possible by the use of the newer NACA 6-series airfoils.

The effect of Reynolds number upon the minimum drag of the NACA 65_4-421 airfoil section is illustrated in figure 8. The data show that the drag first decreases with increasing Reynolds number, after which it levels off, then increases, and finally levels off again as the Reynolds number is further increased. The behavior of the minimum drag with increasing Reynolds number can be attributed to the variation in relative strength of two interacting boundary-layer changes. The initial decrease in minimum drag coefficient can be explained by the usual decrease in skin-friction coefficient which accompanies an increase in Reynolds number. After a certain Reynolds number is reached, however, the transition position begins to move forward along the airfoil. The forward movement of transition, of course, decreases the relative extent of low-drag laminar flow on the airfoil, and hence, the drag increases. The Reynolds number range in which the data in the figure show the drag to be relatively constant is a region in which the general decrease in skin friction and forward movement of transition are balanced with respect to their opposite effects upon the drag. The subsequent increase of drag with Reynolds number indicates that forward movement of transition is predominating in this region. The drag ceases to increase when the transition position comes fairly close to the leading edge. The data in the chart for the highest Reynolds number correspond to this condition. Further increases in Reynolds number should cause the drag coefficient to decrease. The scale-effect curve shown in the figure is characteristic of those obtained for NACA 6-series airfoils. The Reynolds number at which the transition position moves forward, however, depends upon the degree to which the pressure gradients on the airfoil are favorable. The Reynolds number at which the different effects occur depends, therefore, upon the detail design of the particular airfoil.

The development of mean lines designed to shift the low-drag range to different values of the lift coefficient has already been discussed. The effect of the addition of camber on the experimental drag polar is shown in figure 9. (See also reference 7.) The solid curve represents the polar for a symmetrical 6-series airfoil section. The "bucket" in the curve is the low-drag range; that is, the range of lift coefficient through which extensive laminar flow is obtained on both surfaces. As shown by the dash-line curve, the primary effect of the addition of camber is to shift the low-drag range. The center of this range corresponds to the design lift coefficient. The width of the low-drag range increases with increasing airfoil thickness ratio.

The results discussed have been obtained from airfoil tests in which the model surfaces were smooth and fair. Unfortunately, the surfaces of airplane wings are oftentimes both rough and unfair. Since laminar flow cannot be maintained at practical values of the Reynolds number unless the airfoil surfaces are aerodynamically smooth, it seemed desirable to investigate the characteristics of NACA 6-series airfoils with surfaces roughened sufficiently near the leading edge that fully developed turbulent layers would exist. Results corresponding to such a surface condition would give the most pessimistic view of what might be expected from

an airplane wing under any conditions short of physical damage or heavy accretions of ice or mud, whereas the results for the smooth condition would correspond to an optimum for which to strive. The effect of roughness on the lift and drag characteristics of a typical NACA 6-series airfoil section is shown in figure 10. (See also reference 7.) It is apparent that the roughness causes large decreases in the maximum lift and large increases in the drag. Similar data from tests of various types of airfoil sections show that the lift and drag characteristics of airfoils of a given thickness ratio are relatively insensitive to the shape of the basic thickness distributions when the leading edges are rough.

The entire discussion so far has been limited to Mach numbers sufficiently low so that the flow could be considered incompressible. As the Mach number is increased, the first-order effects of compressibility are given by the Prandtl-Glauert relation (reference 20) which states essentially that, in two-dimensional flow, the values of all pressure coefficients formed from differences between local static pressure and free-stream static pressure are increased by the relation $\frac{1}{\sqrt{1 - M_0^2}}$, where M_0 is the free-stream Mach number. This means, of course, that the lift-curve slope is theoretically increased by the same factor, thus,

$$\left(\frac{dc_l}{d\alpha}\right)_c = \frac{\left(\frac{dc_l}{d\alpha}\right)_i}{\sqrt{1 - M_0^2}}$$

where the subscript c indicates compressible flow and the subscript i indicates incompressible flow. A comparison of the theoretical and experimental values of the lift-curve slope for an NACA 6-series airfoil section of 10-percent thickness is shown in figure 11. (See also reference 21.) The expression for the first-order effects of compressibility appears to be valid for thin airfoils up to surprisingly high values of the Mach number. A second-order correction developed by Kaplan (reference 22) gives results in better agreement with experiment at high subcritical values of the Mach number. In general, the increase of lift coefficient with Mach number becomes less as the airfoil thickness ratio is increased, and the agreement between theory and experiment for the thicker sections is less satisfactory.

The effect of compressibility on the drag at speeds below the critical is rather difficult to evaluate. This difficulty arises from the fact that most high-speed test equipment is incapable of separating the effect of increasing Reynolds number which accompanies an increase in Mach number. Some indication of the relative importance of the effect of Mach

number on the drag at subcritical speeds, however, may be gained from figure 12. (See also references 23 and 24.) The drag of the NACA 0012-34 airfoil section at zero lift is plotted against Mach number for a range of Reynolds number from 0.34×10^6 to 0.42×10^6 and for a range of Reynolds number from 2.3×10^6 to 4.6×10^6. The large increment in drag between the high- and low-scale data in the subcritical region is of about the magnitude that would be expected for such a change in the Reynolds number. The data for the higher Reynolds number range are in agreement with recent low-speed tests ($M < 0.2$) of a similar airfoil which show a negligible scale effect on the minimum drag between Reynolds numbers of 3.0×10^6 and 6.0×10^6. From this discussion, it would seem that the effect of Reynolds number is far more important at subcritical speeds than the effect of Mach number. Since in any case the pressure drag is a small part of the total drag, it would not be expected that changes in local-pressure coefficients in accordance with the Prandtl-Glauert relation would have any direct effect upon the drag.

The rather brief summary of the status of the airfoil problem just presented indicates that we have a fairly complete understanding of the behavior of airfoil sections at subcritical speeds. The attainment of laminar flow on airplane wings remains a problem because the surfaces of such wings are usually not sufficiently fair and smooth. Methods of reducing the sensitivity of the laminar layer to surface imperfections are now being investigated. The flow phenomena about an airfoil at maximum lift also remain a problem. We have a qualitative understanding of this problem, but research is needed before our ideas can be extended to quantitative calculation.

REFERENCES

1. Munk, Max M.: The Determination of the Angles of Attack of Zero Lift and of Zero Moment, Based on Munk's Integrals. NACA TN No. 122, 1923.

2. Munk, Max M.: Elements of the Wing Section Theory and of the Wing Theory. NACA Rep. No. 191, 1924.

3. Birnbaum, Walter: Die Tragende Wirbelpläche als Hilfsmittel fur Behandlung des ebenen Problems der Tragflügeltheorie. Z.a.M.M., vol. 3, no. 4, Aug. 1923, pp. 290-297.

4. Glauert, H.: The Elements of Aerofoil and Airscrew Theory. Cambridge Univ. Press, 1926.

5. Theodorsen, Theodore: On the Theory of Wing Sections with Particular Reference to the Lift Distribution. NACA Rep. No. 383, 1931.

6. Jacobs, Eastman N., Ward, Kenneth E., and Pinkerton, Robert M.: The Characteristics of 78 Related Airfoil Sections from Tests in the Variable-Density Wind Tunnel. NACA Rep. No. 460, 1933.

7. Abbott, Ira H., Von Doenhoff, Albert E., and Stivers, Louis S., Jr.: Summary of Airfoil Data. NACA Rep. No. 824, 1945.

8. Theodorsen, Theodore: Theory of Wing Sections of Arbitrary Shape. NACA Rep. No. 411, 1931.

9. Theodorsen, T., and Garrick, I. E.: General Potential Theory of Arbitrary Wing Sections. NACA Rep. No. 452, 1933.

10. Pinkerton, Robert M.: Calculated and Measured Pressure Distribution over the Midspan Section of the N.A.C.A. 4412 Airfoil. NACA Rep. No. 563, 1936.

11. Allen, H. Julian: A Simplified Method for the Calculation of Airfoil Pressure Distribution. NACA TN No. 708, 1939.

12. Jacobs, Eastman N., and Pinkerton, Robert M.: Tests in the Variable-Density Wind Tunnel of Related Airfoils Having the Maximum Camber Unusually Far Forward. NACA Rep. No. 537, 1935.

13. Jacobs, Eastman N., Pinkerton, Robert M., and Greenberg, Harry: Tests of Related Forward-Camber Airfoils in the Variable-Density Wind Tunnel. NACA Rep. No. 610, 1937.

14. Jacobs, Eastman N., and Sherman, Albert: Airfoil Section Characteristics as Affected by Variations in the Reynolds Number. NACA Rep. No. 586, 1937.

15. Jacobs, Eastman N., and Abbott, Ira H.: Airfoil Section Data Obtained in the N.A.C.A. Variable-Density Tunnel as Affected by Support Interference and Other Corrections. NACA Rep. No. 669, 1939.

16. Theodorsen, Theodore: Airfoil-Contour Modifications Based on ϵ-Curve Method of Calculating Pressure Distribution. NACA ARR No. L4G05, 1944.

17. Goldstein, Sydney: Low-Drag and Suction Airfoils. Jour. Aero. Sci., vol. 15, no. 4, April 1948, pp. 189-214.

18. Dryden, Hugh L., and Schubauer, G. B.: The Use of Damping Screens for the Reduction of Wind-Tunnel Turbulence. Jour. Aero. Sci., vol. 14, no. 4, April 1947, pp. 221-228.

19. Von Doenhoff, Albert E., and Abbott, Frank T., Jr.: The Langley Two-Dimensional Low-Turbulence Pressure Tunnel. NACA TN No. 1283, 1947.

20. Glauert, H.: The Effect of Compressibility on the Lift of an Aerofoil. R. & M. No. 1135, British A.R.C., 1927.

21. Graham, Donald J.: High-Speed Tests of an Airfoil Section Cambered to Have Critical Mach Numbers Higher Than Those Attainable with a Uniform-Load Mean Line. NACA TN No. 1396, 1947.

22. Kaplan, Carl: The Effect of Compressibility at High Subsonic Velocities on the Lifting Force Acting on an Elliptic Cylinder. NACA TN No. 1118, 1946.

23. Ferri, Antonio: Completed Tabulation in the United States of Tests of 24 Airfoils at High Mach Numbers (Derived from Interrupted Work at Guidonia, Italy, in the 1.31- by 1.74-Foot High-Speed Tunnel). NACA ACR No. L5E21, 1945.

24. Göthert, B.: Hochgeschwindigkeits-Untersuchungen an symmetrischen Profilen mit verschiedenen Dickenverhältnissen im DVL-Hochgeschwindigkeits-Windkanal (2,7 m Durchm.) und Vergleich mit Messungen in anderen Windkanälen. Forschungsbericht Nr. 1506, Deutsche Luftfahrtforschung, 1941.

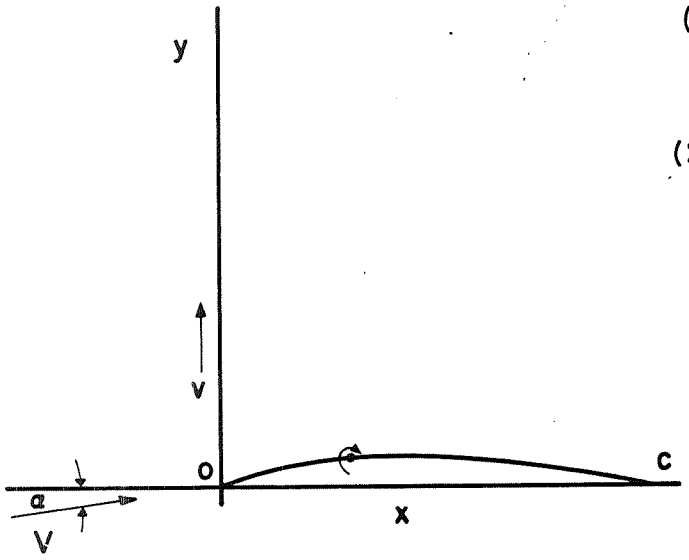

$$(1)\quad \frac{dy}{dx} = \frac{v}{V} - \alpha$$

$$(2)\quad v(x_0) = \int_0^c \frac{\gamma\, dx}{2\pi(x - x_0)}$$

γ = CIRCULATION PER UNIT LENGTH

NACA

Figure 1.- Basic relations of thin-airfoil theory.

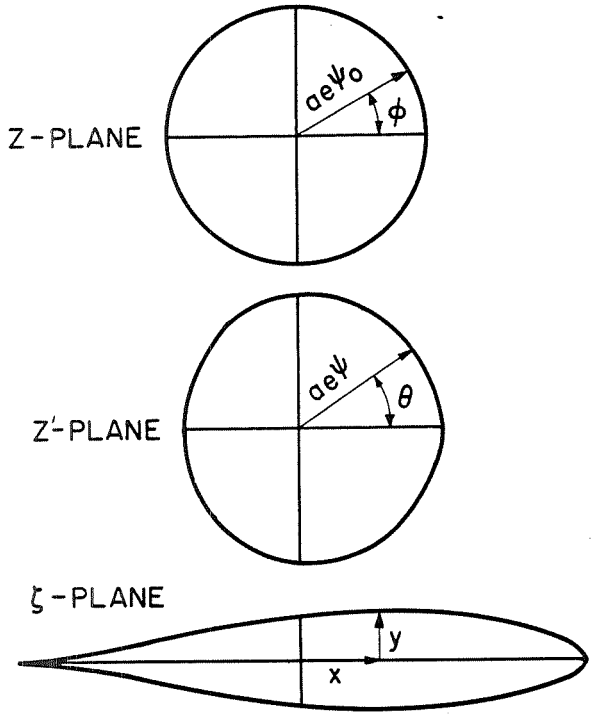

$$Z = ae(\psi_0 + i\phi)$$

$$\frac{Z'}{Z} e[(\psi - \psi_0) + i(\theta - \phi)]$$

$$Z' = ae(\psi + i\theta)$$

$$\zeta = Z' + \frac{a^2}{Z'}$$

NACA

$$\zeta = x + iy$$

Figure 2.- Transformations used to calculate pressure distributions.

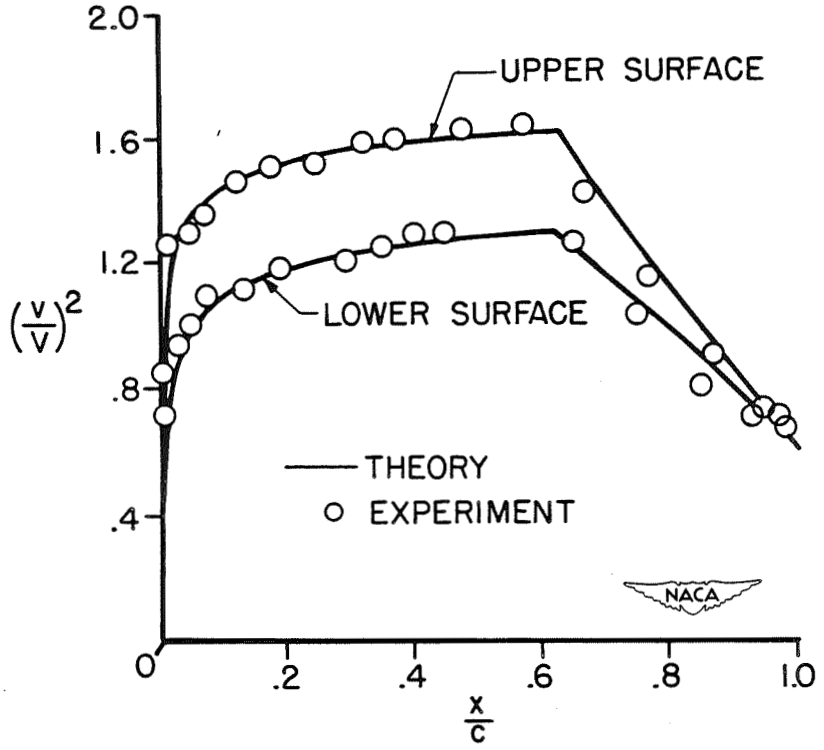

Figure 3.- Comparison of theoretical and experimental pressure distributions.

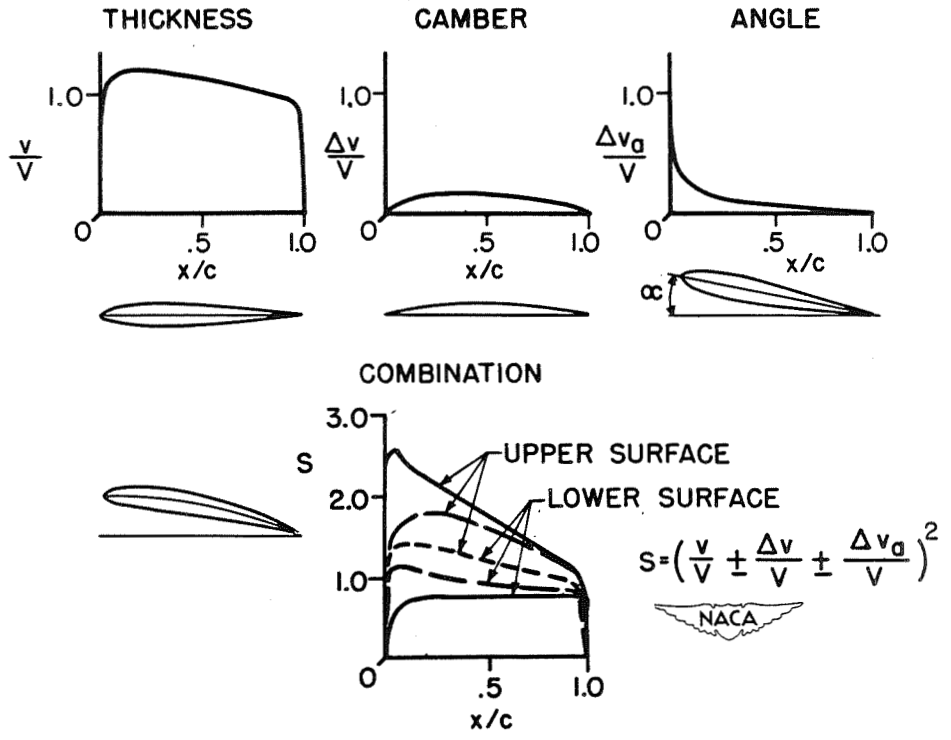

Figure 4.- Synthesis of pressure distribution.

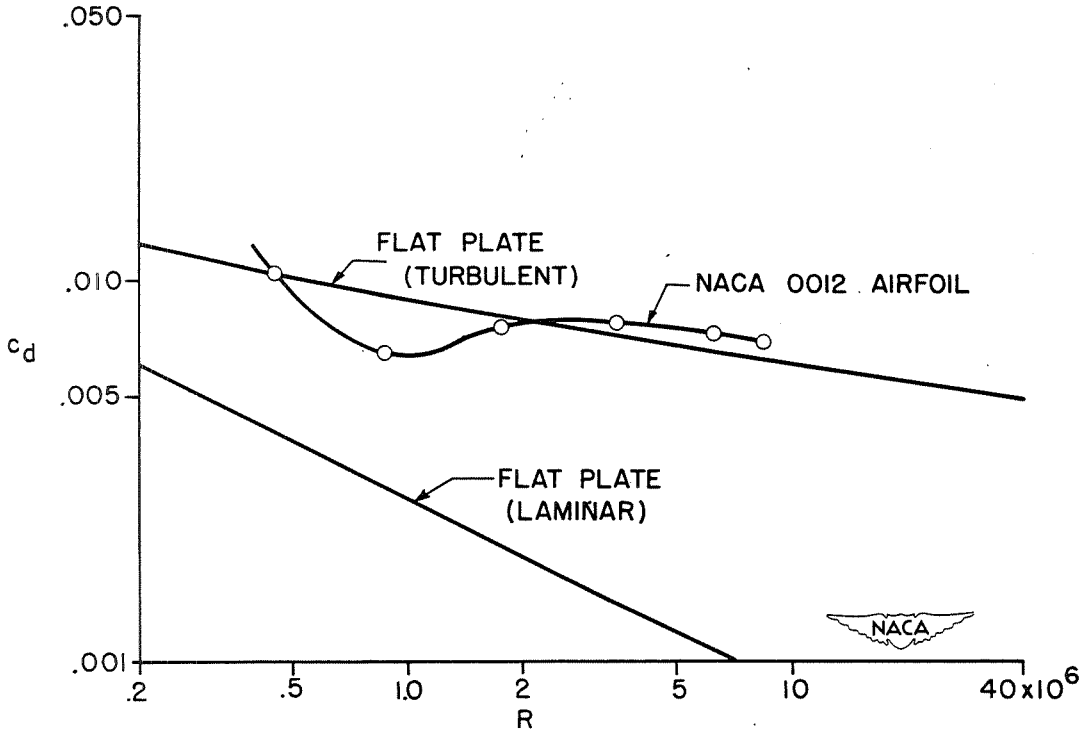

Figure 5.- Section drag coefficient c_d of airfoil and flat plate plotted as function of Reynolds number R.

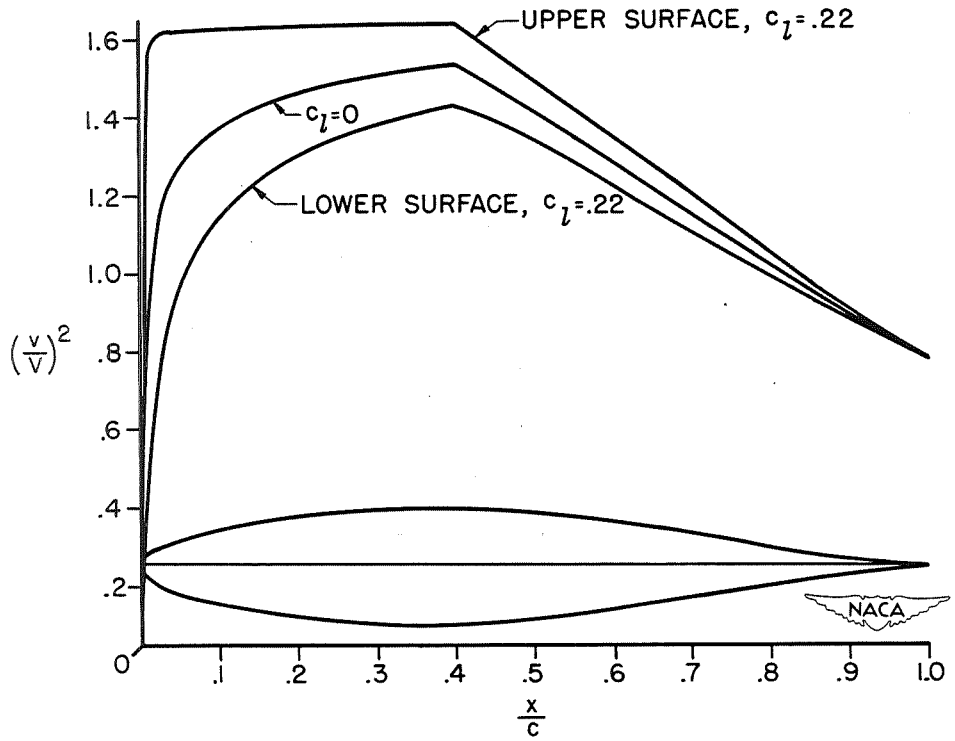

Figure 6.- Pressure distribution for NACA 64_2-015 airfoil section.

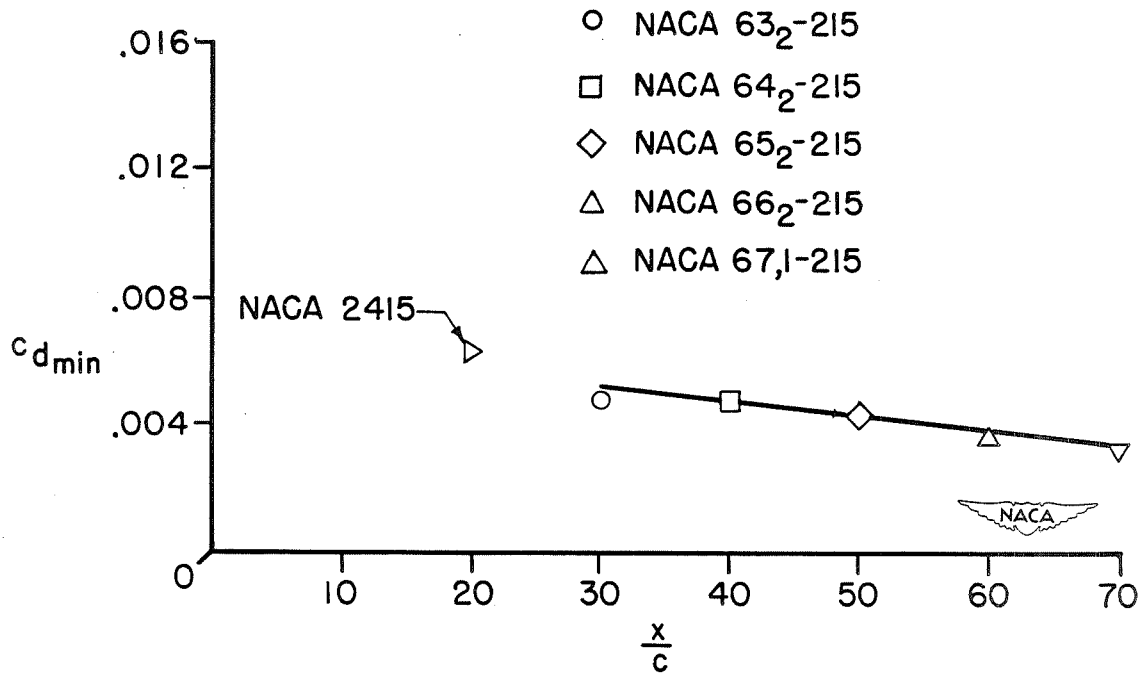

Figure 7.- Variation of minimum drag coefficient $c_{d_{min}}$ with position of minimum pressure x/c.

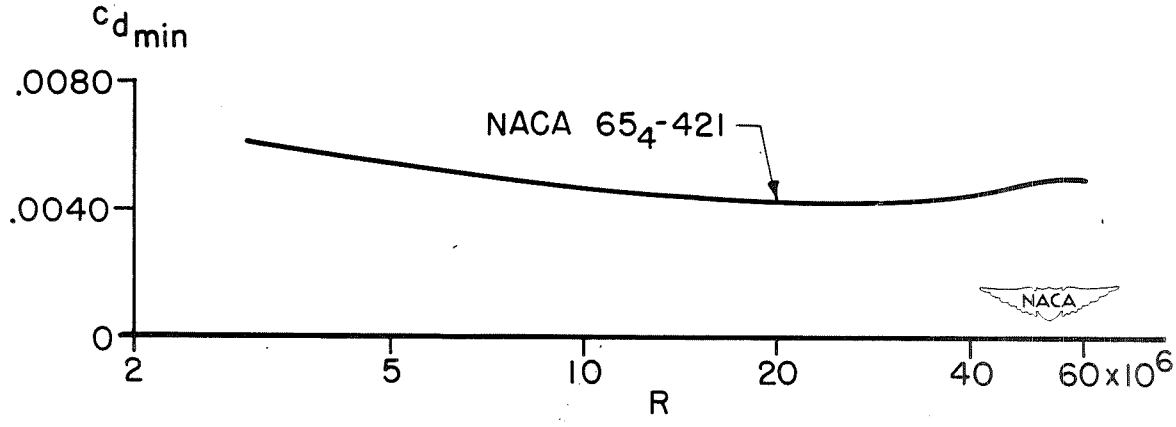

Figure 8.- Effect of Reynolds number on the minimum drag of the NACA 65_4-421 airfoil section.

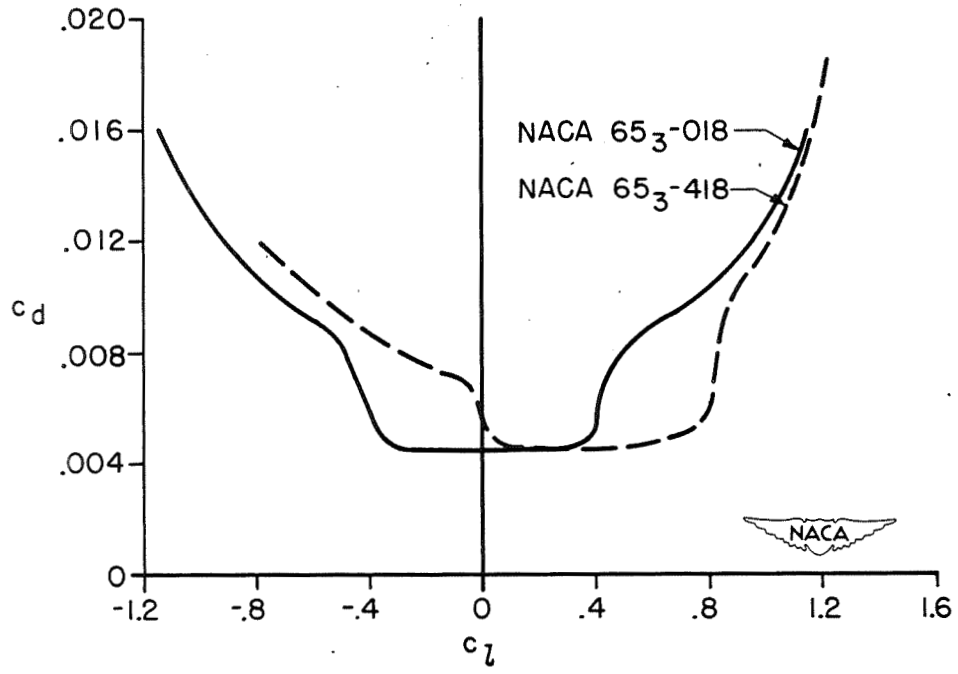

Figure 9.- Effect of camber on the experimental drag polar.

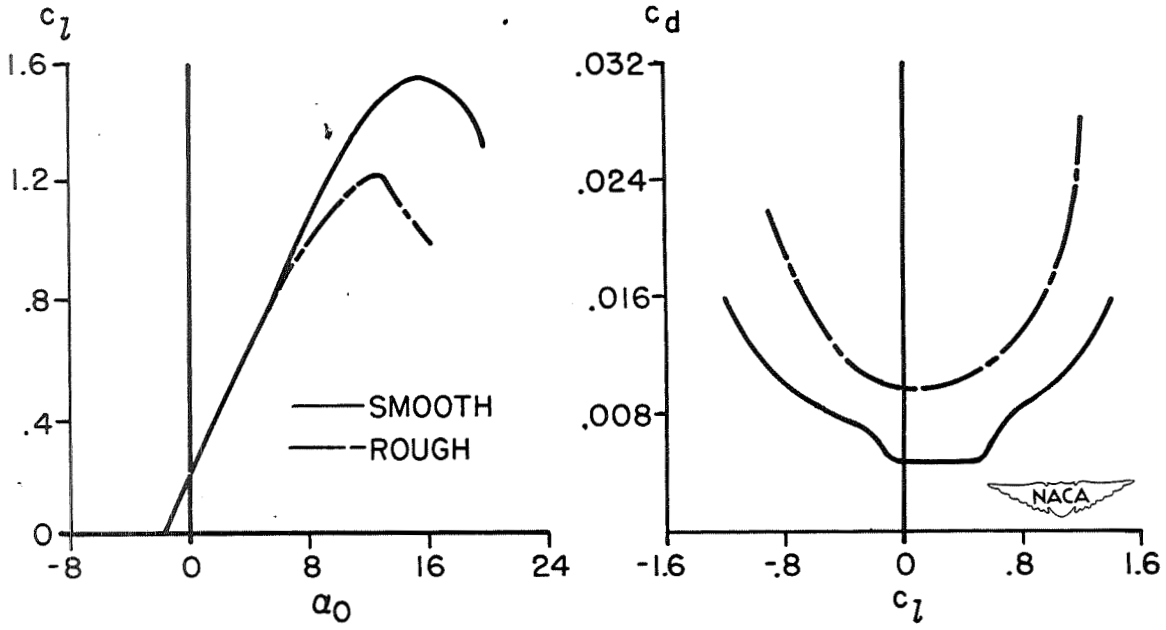

Figure 10.- Effect of roughness on the lift and drag characteristics of a typical NACA 6-series airfoil section.

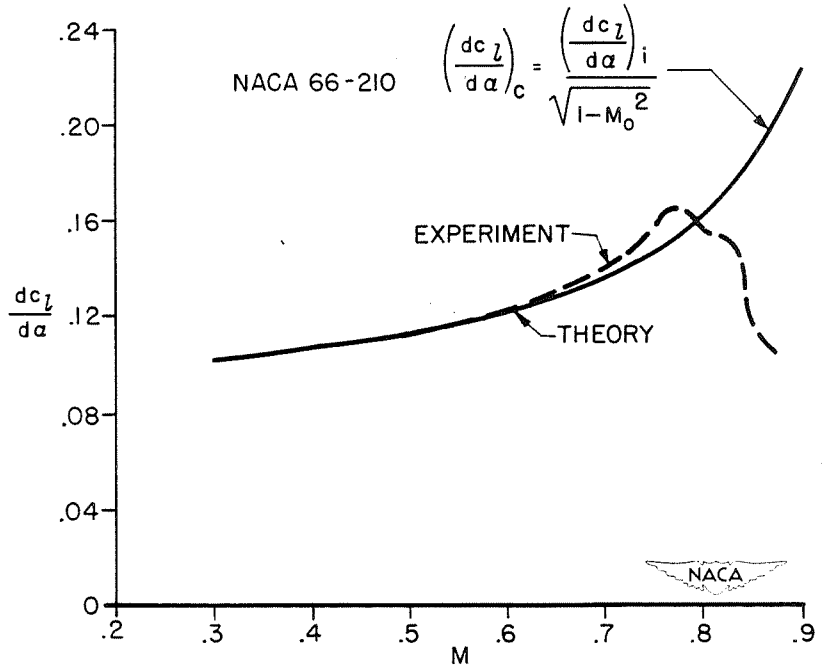

Figure 11.- Comparison of the theoretical and experimental values of the lift-curve slope for an NACA 6-series airfoil section of 10-percent thickness.

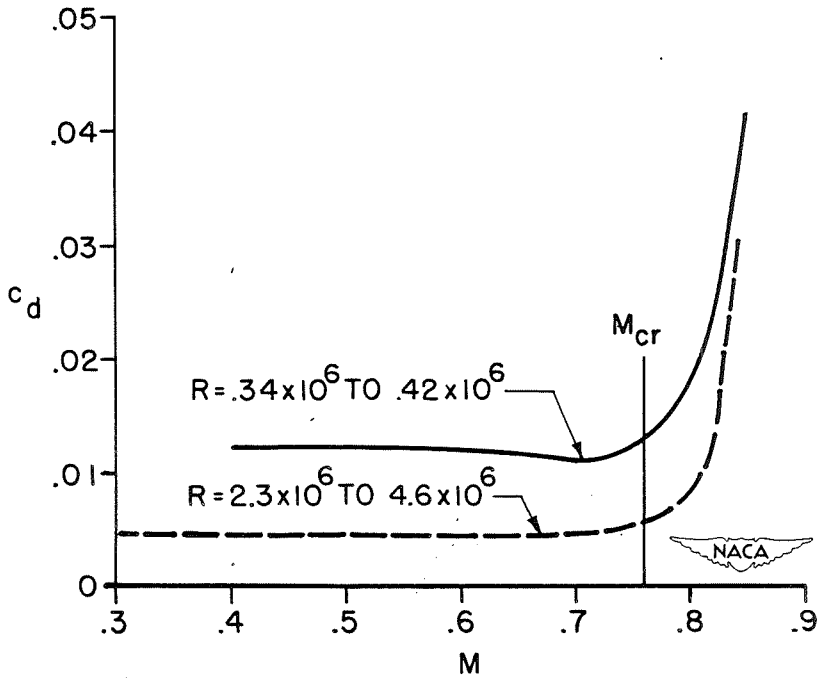

Figure 12.- Effect of Mach number on drag of NACA 0012-34 airfoil section at zero lift.